A novel all-nitrogen molecular crystal N16 as a promising high-energy density material

Journal:	*Dalton Transactions*
Manuscript ID	DT-ART-03-2022-000820.R2
Article Type:	Paper
Date Submitted by the Author:	20-May-2022
Complete List of Authors:	Zhao, Lei; Southwest Petroleum University, Liu, Shijie; Henan University of Science and Technology, Henan Key Laboratory of Photoelectric Energy Storage Materials and Applications,School of Physics and Engineering, Henan University of Science and Technology Chen, Yuanzheng; Southwest Jiaotong University, School of Physical Science and Technology Yi, Wencai; Qufu Normal University, Laboratory of High Pressure Physics and Material Science Khodagholian, Dalar ; California State University Northridge, b. Department of Chemistry & Biochemistry Gu, Fenglong; South China Normal University Kelson, Eric; California State University Northridge Zheng, Yonghao; University of Electronic Science and Technology of China, Liu, Bingbing; Jilin University, State Key Laboratory of Superhard Materials Miao, Mao; California State University Northridge

A novel all-nitrogen molecular crystal N$_{16}$ as a promising high-energy density material

Lei Zhao[1,2∥], Shijie Liu[3,4∥], Yuanzheng Chen[5], Wencai Yi[6], Darlar Khodagholian[2],

Fenglong Gu[7], Eric Kelson[2], Yonghao Zheng[8]*, Bingbing Liu[4]*, Mao-sheng Miao[2,9]*

[1] College of Chemistry and Chemical Engineering, Southwest Petroleum University, Chengdu 610500, P. R. China

[2] Department of Chemistry & Biochemistry, California State University Northridge, Northridge, CA, 91330, United States

[3] School of Physics and Engineering, and Henan Key Laboratory of Photoelectric Energy Storage Materials and Applications, Henan University of Science and Technology, Luoyang 471003, P. R. China

[4] State Key Laboratory of Superhard Materials, Jilin University, Changchun 130012, P. R. China

[5] School of Physical Science and Technology, Key Laboratory of Advanced Technologies of Materials, Ministry of Education of China, Southwest Jiaotong University, Chengdu 610031, P. R. China

[6] School of Physics and Physical Engineering, Qufu Normal University, Qufu, 273165, P. R. China

[7] Key Laboratory of Theoretical Chemistry of Environment, Ministry of Education, School of Chemistry and Environment, South China Normal University, Guangzhou 510006, P. R. China

[8] School of Optoelectronic Science and Engineering, University of Electronic Science and Technology of China (UESTC), Chengdu 610054, P. R. China

[9] Beijing Computational Science Research Center, Beijing, 100193, P. R. China

ABSTRACT: All-nitrogen solids, if successfully synthesized, are ideal high energy density materials because they store a great amount of energy and produce only harmless N_2 gas upon decomposition. Currently, the only method to obtain all-nitrogen solids is to apply high pressure to N_2 crystals. but the products such as cg-N tend to decompose after releasing the pressure. Compared to covalent solids, molecular crystals are more likely to remain stable during decompression because they can relax the strain by increasing intermolecular distances. The challenge of such a route is to find a molecular crystal that can become a favorable phase under elevated pressure. In this work, we show, by designing a novel N_{16} molecule (tripentazolylamine) and searching its crystal structures under a series of pressures, that the aromatic units and high molecular symmetry are the key factors of achieving an all-nitrogen molecular crystal. Density functional calculations and structure searches reveal that this new all-nitrogen molecular crystal exhibits a particularly slow enthalpy increase with pressure due to the highly efficient crystal packing of these highly symmetric molecules. Vibration mode calculations and molecular dynamics (MD) simulations show the N_{16} crystal is metastable at ambient pressure and could remain inactive up to 400 K. The initial reaction steps of the decomposition are calculated following the pathway of concerted excision of N_2 from N_5 group revealed by MD simulations.

INTRODUCTION

Nitrogen rich compounds are promising high energy density materials, not only because they can release great amounts of energy upon decomposition[1,2], but also because their major gas product, diatomic nitrogen (N_2), is inert. non-toxic, and non-polluting. The large energy release comes from the fact that the triple bond ($N\equiv N$) of N_2 has the greatest binding energy (~226 kcal mol^{-1}) among all molecules[3,4]. For these reasons, an all-nitrogen solid would be an ideal high energy density material. However, these materials have proven to be difficult to produce and stabilize. For example, the aromatic pentazolate anion N_5^- (with 6 electrons in its conjugated pi system) traditionally requires binding with organic functional groups to be maintained in a controllable metastable state and has only been successfully realized recently by organic synthetic methods[5-11]. Alternatively, exciting progress has been made in high-pressure studies showing that many metal pentazolates are thermodynamically stable under high pressure[12-17]. Recent experiments have demonstrated that lithium pentazolate produced at high pressure could be recovered upon the release of pressure down to atmospheric conditions. However, most of the pentazolate compounds, with very rare exceptions[18], contain metals and/or organic groups that lower the energy density and contribute to undesired products upon decomposition. The goal of obtaining metastable all-nitrogen compounds remains unfulfilled.

4

While applying the concept of high-pressure synthesis to all-nitrogen compounds, we encounter a fundamental difficulty: aside from N_2 crystals, nitrogen compounds are either not thermodynamically stable throughout the pressure range or cannot be recovered in a controllable metastable form at ambient conditions[19-24]. At lower pressure, the stable forms of nitrogen are N_2 molecular crystals in various lattice arrangements[25-27]. The first stable high-pressure form of nitrogen is the "cubic gauche" (cg)-N that was first predicted by Mailhiot et al.[28] to form at pressures above 60 GPa and subsequently confirmed by Eremets et al.[29] in DAC experiments at about 110 GPa. Many other polymeric nitrogen materials also have been predicted[30-33] including a diamondoid N_{10} structure that becomes the most stable form of nitrogen at pressures above 263 GPa. All of these high-pressure forms of nitrogen consist of extended N-N covalent networks. Unfortunately, these extended structures of nitrogen cannot be recovered and maintained in a metastable state at ambient conditions because the N-N bonds largely stretch away from their equilibrium length as high pressure is released and reorganize into N_2 molecules.

The above results suggest that a more productive search for all-nitrogen high-energy materials would focus on all-nitrogen molecular crystals rather than extended solids. The crystals of all-nitrogen molecules, small or large, can more easily adapt to atmospheric pressure conditions by increasing the inter-molecular distances and avoiding significant deviations of intra-molecular N-N or N=N lengths from their equilibrium values. So far, high-pressure methods remain the most feasible means to

producing such materials. However, in order to apply such a methodology, the proposed all-nitrogen compound needs to be, in a specific pressure range, either thermodynamically stable or in a metastable structure not much higher in enthalpy and be connected to the precursor state within a structure subspace constrained by kinetic barriers. Generally speaking, we need to find an all-nitrogen molecular crystal that is low in energy at ambient conditions (1 atm), and has a low enthalpy increase rate while applying pressure. Ideally, the H-P curve of this compound can intercept the H-P curve of a N_2 phase before it intercepts that of the cg-N.

The idea of computationally searching for promising all-nitrogen molecules is not new, and numerous candidates have been predicted by quantum chemistry calculations[34-42]. However, these studies neglect the arrangement of these molecules in crystals and the consequential response to pressure, largely due to the difficulties in predicting the crystal structures of specific molecules. A few exceptions include the linear N_8 molecule whose crystal structure was recently reported[43] and our recent work that predicts the crystal structure N_{10} molecules[44]. Calculations showed that the enthalpy of crystalline N_8 increases quickly with increasing pressure and exceeds that of cg-N at about 20 GPa, a pressure that is much lower than the transition pressure (~50 GPa) from ε-N_2 to cg-N. The rapid increase in enthalpy with pressure for crystalline N_8 is caused by the inefficient packing of these low symmetry molecules. This geometric consideration poses a dilemma: larger nitrogen molecules possess more N-N and/or

N=N bonds and store more energy, but they also pack poorly into crystals resulting in low stability under high pressure.

In this work, we put forward a new all-nitrogen N_{16} molecule consisting of three N_5 rings connecting to a center N atom that captures the advantages of size and good crystal packing. This molecule maximizes aromaticity and is therefore low in energy. Using a structure search method based on particle swarm intelligence[45], we identified the most likely crystal structure that features efficient packing of N_{16} as a result of its high molecular symmetry. Further first-principles calculations revealed that this compound is low in energy at ambient conditions and its enthalpy increases at a relatively low rate with increasing pressure. Although crystalline N_{16} still does not become globally stable under high pressure, its enthalpy is much closer to those of cg-N and N_2 around their transition point. This work demonstrates that all-nitrogen molecular crystals could be prepared by high-pressure techniques if molecular and crystal structures are both optimized. We also demonstrate in this work that electron doping can stabilize N_{16} such that it can become thermodynamically stable under high pressure.

METHODS

Molecular structure searches are performed using the CALYPSO code with the local PSO minimization schemes[46]. Local structural relaxations are performed by density functional theory as implemented in the Vienna ab initio simulation package (VASP code)[47,48]. The electron-electron interaction was treated with a generalized gradient approximation (GGA) parametrized by Perdew-Burke-Ernzerhof (PBE) functional[49].

Projector-augmented-wave (PAW) was employed to describe the interaction between valence electrons and the core[50,51]. To describe the intermolecular interaction of molecular structured material, the van der Waals interaction of the optB88-vdW method was added in calculations[52,53]. Electronic wave functions are expanded with plane waves up to a kinetic energy cutoff of 500 eV. The geometries were optimized using the conjugate gradients (CGs) scheme until the force components on each atom were less than 0.01 eV $Å^{-1}$, and the self-consistent field calculations were stopped when energy was smaller than 1×10^{-8} eV $atom^{-1}$. Brillouin zone (BZ) integrations were performed using a Gamma centered k-point mesh of $5 \times 3 \times 6$. A phono spectrum was calculated to examine dynamical stability, with a $2 \times 2 \times 1$ supercell using the PHONOPY package[54]. The canonical ensemble (NVT) was implemented in molecular dynamics simulations with a large $2 \times 2 \times 1$ supercell containing about 128 atoms to check the thermal stability. All the molecular geometry optimization and transition state calculation were performed with Gaussian 16 software at B3LYP/6-31G(d) level[55-58].

RESULTS AND DISCUSSION

The proposed N_{16} molecule consists of three N_5 units that are isoelectronic to N_5^-. The N_5^- ion has 26 valence electrons (25 from the 5 N atoms and 1 from the charge), 10 of which occupy the bonding states of the five σ bonds in the ring and another 10 represent the 5 lone pairs. The remaining electrons occupy the π orbitals and apparently follow the 4n+2 Hückel Rule for aromaticity (n=1). Thus the N_5^- unit, as suggested by Schleyer et. al.[59,60], is a fundamental stable all-nitrogen unit. The N_{16} molecule brings

three of these N_5^- units together by replacing three H atoms in NH_3 (Figure 1a), and thus named tripentazolylamine. It is important to emphasize that the tripentazolylamine molecule is not aromatic and the central nitrogen in N_{16} is bent like that in ammonia. It features a dihedral angle of 24.35° between the central nitrogen atom and three neighboring nitrogen atoms. This is in contrast to triphenylamine in which the central N and the three neighboring C atoms are in the same plane corresponding to a dihedral angle of 0°. Although the delocalization of the lone pair electrons on the central N atom contribute to the stabilization of the whole molecule, the central N is between sp^2 and sp^3 hybridization because of the spatial repulsion. The electronic structure calculations of N_{16} show that all of the N atoms in this N_{16} molecule are close to neutral by NBO charge calculation and the number of π electrons on each N_5^- ring satisfies the 4n+2 rule of aromaticity. Vibration mode calculations show no negative frequencies for the optimized N_{16} molecule structure, confirming that N_{16} can remain metastable as an isolated molecule (Table S1).

To evaluate the stability of the N_{16} molecule, its energy was calculated and compared to those of many previously proposed all-nitrogen molecules N_n (2 $\leq$ n $\leq$ 20). The calculated energies with zero-point energy correction are shown in Figure 1b. Among these N_n molecules, N_2 molecule is most energetically stable due to its triple bond. Besides N_2, the molecules bearing N_5 rings (N_{16}, N_{12}[38], and N_{14}[39] – the latter two linking the rings with one or two N=N units) show relatively low energies. In addition to these molecules, the previously studied linear-N_6[35] and recently proposed N_8-EZE[43]

molecules also have energies close to N_{16}. Although many high symmetry all-nitrogen

molecules such as the cubic N_8[36] and tetragonal N_4[34] are quite high in energy relative

to N_{16}, they can efficiently pack in a crystal and might assume significantly smaller

volumes under high-pressure and exhibit consequently lower strain energies (PV). It is

a major objective of this work to bring high pressure crystal strain energies into

consideration for predicting candidate all-nitrogen molecules.
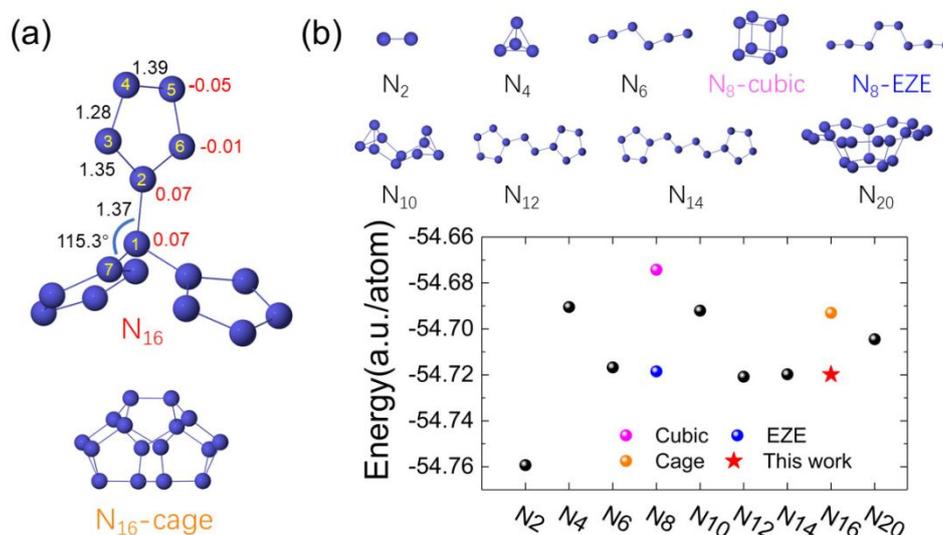
Figure 1. (a) Structures of the proposed N_{16} molecule and previously reported N_{16}-cage

cluster. The black and red color numbers are responding for bond length (Å) or angle

and NBO charges, respectively, (b) Energy sequence of our predicted N_{16} along with

other nitrogen molecules by the energy per atom calculated at B3LYP/6-31G(d) level.

Configurations of N_2, N_4[34], N_6[35], N_8 (EZE[43] and cubic[36]), N_{10}[37], N_{12}[38], N_{14}[39], N_{16} cage[40]

and N_{20}[41] molecules are also provided for clarity.

In order to study the crystal strain energies due to compression, we need the crystal

structures of the all-nitrogen molecules under different pressures. In cases where the

crystal structures were not known (as was the case with N_{16} and cubic N_8), they were predicted through an automatic crystal structure search method based on first principles geometry optimizations and total energy calculations and the use of a particle swarm optimization (PSO) algorithm. The thus predicted crystal structure of N_{16} is shown in Figure 2, together with the crystal structure of linear N_8 conceived in the work of Benny Gerber et al[43].

Only one crystal structure consisting of N_{16} molecules was found in the pressure range from 0 to 100 GPa indicating that there is no pressure-dependent crystal structure change for this compound. The obtained structure consists of 32 N atoms per cell and is in the *Cm* space group (Figure 2a), detailed discussion can be seen in SI (Figure S1). The average N-N bond length between the central nitrogen and pentazole rings stretched slightly in the solid state compared to that in the gas phase. The average angle between pentazole rings also decreased after packing in condensed phase (Table S2). The dihedral angle between the central nitrogen atom and three pentazole nitrogen atoms increases slightly from 24.35° in the gas phase to 25.75° in the solid phase. The optimized lattice parameters for this structure are provided in Table S3. The structure shows efficient packing for N_{16} molecules, not only because the N_{16} molecules are highly symmetric, but also because the tridendritic geometry allows a good filling of the space between neighboring molecules. The effective packing of N_{16} molecules suggests that its crystal might have lower strain energy and become more stable than other all-nitrogen molecular crystals under high pressure. The formation energy of N_{16}

in the gas and solid states were calculated (Table S4). At 0GPa the value for the solid

state (12.799 eV) significantly decreased from that in gas phase (17.178eV). Although

the formation energy is positive at 0GPa, it is negative when the pressure is higher than

80GPa. This suggests that synthesis under high pressure is possible.
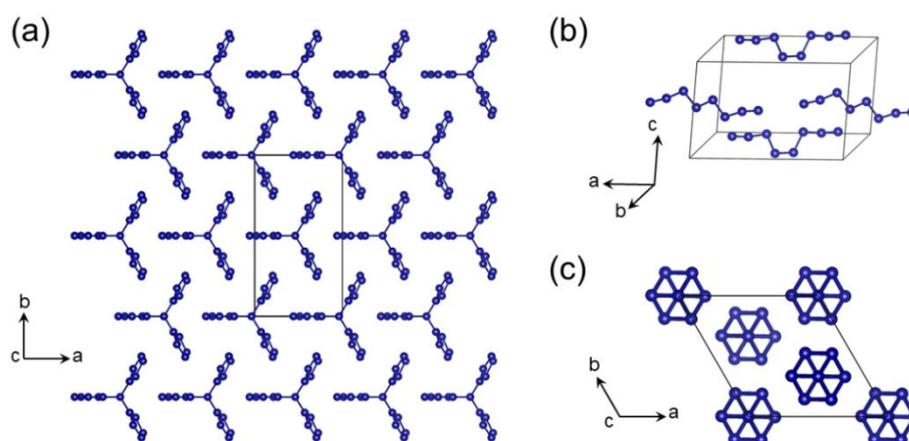
Figure 2. Crystal structures of (a) predicted N_{16} crystal, (b) the reported N_8 crystal

structure and (c) predicted cubic-N_8 crystal structure.

To check the dynamic stability of this N_{16} crystal, its phonon band structure along

high symmetry line was calculated. As shown in Figure S2, no imaginary frequencies

were found, confirming its dynamic stability. In order to examine its thermal stability,

we performed *ab initio* molecular dynamics (AIMD) simulations for 6 ps containing

4000 MD steps at temperatures up to 350 K. No sign of dissociation to N_{16} molecules

in the crystal, which indicates the good stability of this new nitrogen molecular crystal.

The final configuration and energy changes for molecular dynamic simulation are shown in Figure S3.

The crystal enthalpies of N_{16} were compared with those of linear and cubic N_8, cg-N, ε-N_2, and dimondoid-N_{10} under a series of pressures up to 100 GPa (Figure 3a). Under 0 GPa, crystalline N_{16} is the most stable among the studied all-nitrogen materials except ε-N_2 itself. The crystal enthalpy of linear N_8 is only modestly higher (0.048 eV atom^{-1}) than that of N_{16} crystals while that of cubic N_8 is significantly greater (1.13 eV atom^{-1}). Further, crystalline N_{16} is significantly lower in energy than the extended all-nitrogen solids (0.52 eV atom^{-1} and 1.21 eV atom^{-1} for cg-N and diamondoid-N solids, respectively). On the other hand, crystalline N_{16} is 0.80 eV atom^{-1} higher in energy than ε-N_2 which represents the large potential energy stored in the N_{16} crystal.
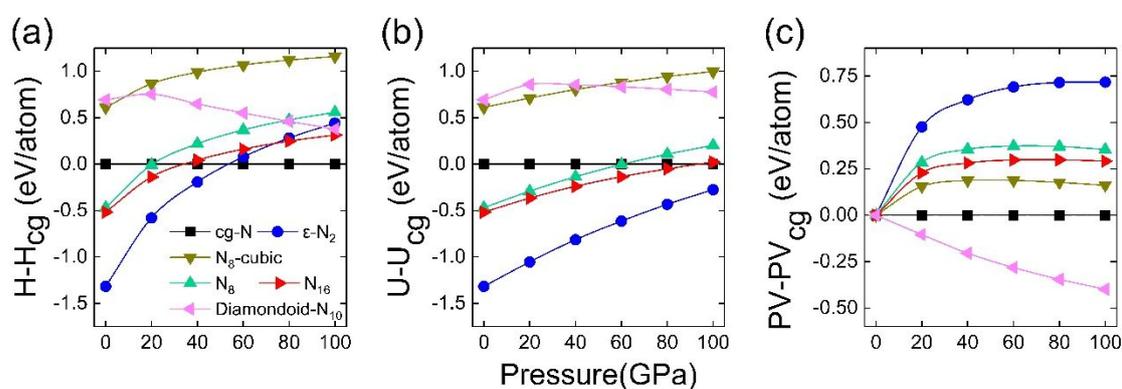
Figure 3. Pressure dependence of the (a) enthalpy, (b) internal energy and (c) PV difference per atom of the N_{16} crystal and some typical nitrogen crystalline solid relative to the experimentally synthetized cg-N_2.

As external pressure increases, the enthalpies for the molecular crystals increase faster than the extended solids (cg-N and diamondoid-N). However, among all the molecular crystals, N_{16} is the one that shows the slowest enthalpy increase with pressure. The enthalpy of N_{16} under pressure shows two important cross points as pressure increases. At 40 GPa, it becomes higher than that of cg-N, and at 80 GPa, it becomes lower than that of ε-N_2. Because cg-N becomes more stable than ε-N_2 at 53.6 GPa, there is no pressure range that N_{16} is the most stable allotrope. However, N_{16} is the most stable all-nitrogen molecular crystal under high pressure. At 53.6 GPa, it is 0.128 eV atom^{-1} higher than cg-N and ε-N_2, significantly lower than that of 0.327 eV atom^{-1} for linear N_8. Interestingly, electron doping (perhaps from metal incorporation) can make crystalline N_{16} thermodynamically stable under high pressure. When 0.75% extra electrons (i.e. 0.6 electron per N_{16} molecule) are doped into crystal models, N_{16} becomes more stable than cg-N up to 80GPa and is only 0.089 eV atom^{-1} higher in enthalpy over cg-N at 100GPa (Figure 4).
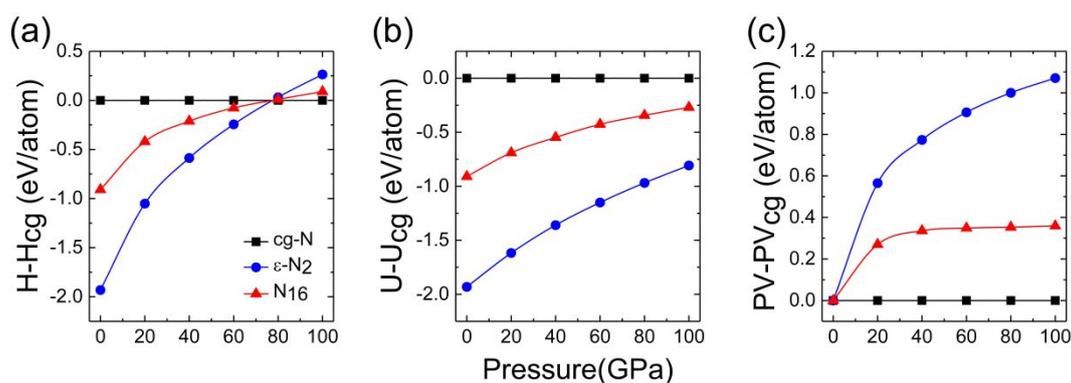
Figure 4. Pressure dependence of the (a) enthalpy, (b) internal energy and (c) PV difference per atom of the N_{16} and ε-N_2 crystal relative to the experimentally synthetized cg-N_2 with 0.75% extra electrons.

To understand the pressure induced stability changes for the all-nitrogen materials and the underlying mechanisms, the crystal internal energies (Figure 3b) and PV terms (Figure 3c) were calculated. Figure 3b reveals that the internal energies for the molecular crystals increase almost linearly relative to that of cg-N under increasing pressure, and this is the major driving force destabilizing them. It is interesting that, among all the molecular crystals, the internal energy of N_{16} increases slowest. This is largely due to the aromaticity of the N_5 units in N_{16} molecules. On the other hand, the contribution of the PV term is less significant and does not always change monotonically with increasing pressure. The PV terms for the molecular crystals relative to cg-N increase rapidly at lower pressures. However, they reach a plateau around 20 GPa indicating that the compressibility of molecular crystals and cg-N become similar beyond 20 GPa. Among all the molecular crystals, cubic N_8 and N_{16} have the lowest PV due to efficient packing within their crystal structures. Of the molecular all-nitrogen materials, crystalline N_{16} distinguishes itself for having the slowest increase in the crystal internal energy and PV term as a result of its aromatic units and efficient crystal packing.

A good high energy material not only needs to store a large quantity of energy but also needs to maintain stability and release the energy in a controlled fashion. The latter

two qualities are determined by the decomposition pathways and kinetic barriers. While

calculation of a full energy landscape for such a complex material is impractical,

molecular dynamic simulations can provide a good estimation of its stability. We

performed AIMD calculations on canonical ensembles with large supercells containing

about 128 atoms at 400K, 800K, and 1000K, respectively. Figures 5a-5c depict total-

energies as functions of the simulation steps as well as the final equilibrium structures

at each temperature. These simulations exhibit stepwise curves corresponding to steps

in the decomposition pathway. The simulation at 400 K features a single significant

step representing the initiatory dissociation of one of the three N_5 units in each N_{16}

molecule to N_3 and N_2. At 800 K, the energy curve shows two distinct steps for the

cleavage of two N_5 units to N_3 and N_2 in each N_{16} molecule. At 1000 K, the energy

progressively decreases with no obvious intermediate stages, and all the N_5 units in the

crystal are decomposed by the end of the simulation. The decomposition pathway of

pentazole has been studied[61], and results show that the pentazole ring prefers to lose a

nitrogen molecule to form azide, this is the same as what we found in N_{10}[44] and N_{16}

molecular crystal decomposition.

Inspired by the AIMD simulations on the decomposition processes in N_{16} crystals,

we investigated the decomposition pathway of the N_{16} molecule using a DFT method

at the B3LYP/6-31G(d) level. The schematic potential energy surfaces for

decomposition products and transition states (TS) of the N_{16} molecule are illustrated in

Figure 5d. As predicted by the AIMD simulations, it is clear that the decomposition of

the N_{16} molecules begins with the concerted excision of N_2 from the N_5^- rings and progresses with the sequential opening of all three N_5^- rings. Our DFT calculations show that the transition barriers of the three ring opening processes are 7.1 kcal mol^{-1} for TS1 $[N(N_5)_3 \rightarrow TS1 \rightarrow N(N_5)_2N_3+N_2]$, 4.8 kcal mol^{-1} for TS2 $[N(N_5)_2N_3 \rightarrow TS2 \rightarrow NN_5(N_3)_2+2N_2]$, and 6.6 kcal mol^{-1} for TS3 $[NN_5(N_3)_2 \rightarrow TS3 \rightarrow N(N_3)_3+3N_2]$. The low barriers for these reaction steps concur with the AIMD simulations that the N_{16} crystal can easily release its energy along a well-defined initiation pathway.
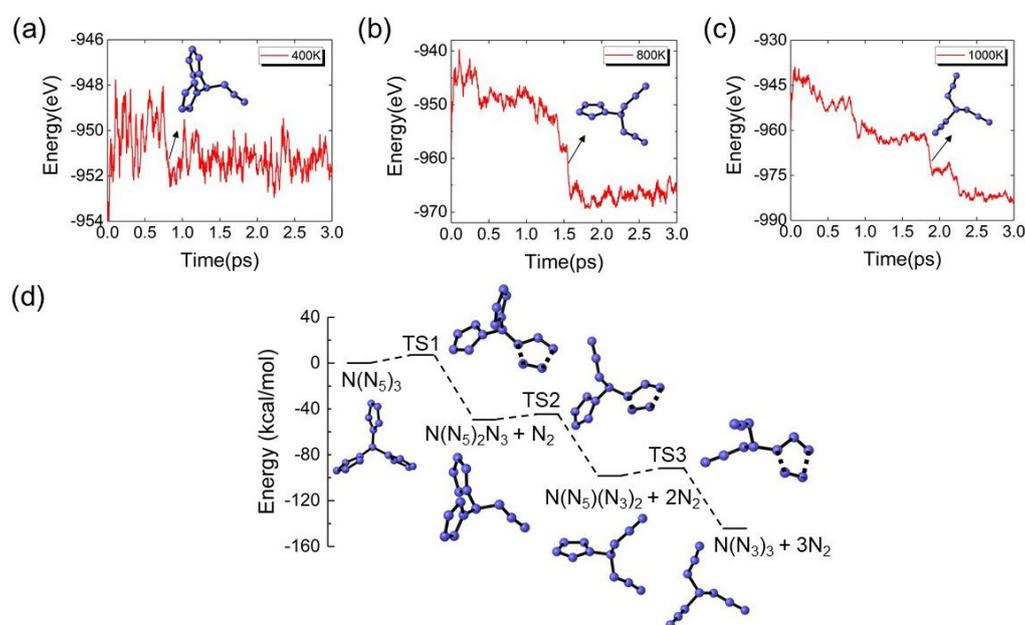
Figure 5. The structure and total-energy evolution for a N_{16} crystal in AIMD simulations at different temperature 400K (a), 800K (b), and 1000K (c), respectively; (d) the energy profile of N_{16} molecular decomposition at the B3LYP/6-31G(d) level.

In conclusion, we propose a new all-nitrogen high-energy density material formed by effective crystal packing of N_{16} molecules consisting of three linked aromatic N_5^- rings. The combination of high molecular symmetry and aromaticity leads to

17

superlative properties. At atmospheric pressure, N_{16} is the lowest energy all-nitrogen compound aside from molecular N_2 itself. Among molecular all-nitrogen materials, the crystal enthalpy of N_{16} increases slowest with increasing pressure due to its high packing efficiency such that it becomes more stable than ε-N_2 near 80 GPa. Although the polymeric cg-N still is the most stable high-pressure form of all-nitrogen compounds, the favorable low energy, dynamic stability, and slow crystal enthalpy increase with pressure for crystalline molecular N_{16} makes it a potential candidate as an all-nitrogen high energy density material. The demonstration of such a material that combines the low energy metastability at atmospheric pressure and the low enthalpy increasing rate shows that high pressure might be a promising route toward finding all-nitrogen energy materials.

ASSOCIATED CONTENT

Supporting Information

Harmonic vibrational analysis of N_{16} molecule; geometries of N_{16} in gas phase and solid state; structure parameters for N_{16} crystal; formation energy of N_{16} in the gas phase and solid state; symmetry discussion of N_{16} crystal; phonon dispersion of N_{16} crystal; energy change and snapshots of the final configurations for AIMD simulation of N_{16} crystal at 350K.

AUTHOR INFORMATION

Corresponding Authors

* Email: mmiao@csun.edu

* Email: liubb@jlu.edu.cn

* Email: zhengyonghao@uestc.edu.cn

‖Lei Zhao and Shijie Liu made equal contribution to this work.

Notes

ACKNOWLEDGMENT

REFERENCES

1   Nellis, W. *et al.* Equation-of-state, shock-temperature, and electrical-conductivity data of dense fluid nitrogen in the region of the dissociative phase transition. *J Chem Phys* **94**, 2244-2257 (1991).

2   Martin, R. M. & Needs, R. J. Theoretical study of the molecular-to-nonmolecular transformation of nitrogen at high pressures. *Phys Rev B* **34**, 5082 (1986).

3   Samartzis, P. C. & Wodtke, A. M. All-nitrogen chemistry: how far are we from N_{60}? *Int Rev Phys Chem* **25**, 527-552 (2006).

4   Young, D. A. *Phase diagrams of the elements.* (Univ of California Press, 1991).

5   Xu, Y. *et al.* A series of energetic metal pentazolate hydrates. *Nature* **549**, 78 (2017).

6   Zhang, C., Sun, C., Hu, B., Yu, C. & Lu, M. Synthesis and characterization of the pentazolate anion cyclo-N_5 in $(N_5)_6(H_3O)_3(NH_4)_4Cl$. *Science* **355**, 374-376 (2017).

7   Zhang, C. *et al.* A Symmetric $Co(N_5)_2(H_2O)_4 \cdot 4H_2O$ High-Nitrogen Compound Formed by Cobalt (II) Cation Trapping of a Cyclo-N_5^- Anion. *Angew Chem Int Edit* **56**, 4512-4514 (2017).

8   Xu, Y., Wang, P., Lin, Q., Mei, X. & Lu, M. Self-assembled energetic 3D metal-organic framework $[Na_8(N_5)_8(H_2O)_3]_n$ based on cyclo-N_5^-. *Dalton T* **47**, 1398-1401 (2018).

9   Xu, Y., Lin, Q., Wang, P. & Lu, M. Stabilization of the Pentazolate Anion in

       Three Anhydrous and Metal-Free Energetic Salts. *Chemistry-An Asian Journal*

       13, 924-928 (2018).

10   Wang, P.-C. *et al.* Self-assembled energetic coordination polymers based on

       multidentate pentazole cyclo-N_5^-. *Sci China Mater* **62**, 122-129 (2019).

11   Xu, Y., Wang, P., Lin, Q. & Lu, M. A carbon-free inorganic-metal complex

       consisting of an all-nitrogen pentazole anion, a Zn (II) cation and H_2O. *Dalton*

       T **46**, 14088-14093 (2017).

12   Peng, F., Yao, Y., Liu, H. & Ma, Y. Crystalline LiN_5 predicted from first-

       principles as a possible high-energy material. *J Phys Chem Lett* **6**, 2363-2366

       (2015).

13   Shen, Y. *et al.* Novel lithium-nitrogen compounds at ambient and high

       pressures. *Sci. Rep.* **5**, 14204 (2015).

14   Li, J., Sun, L., Wang, X., Zhu, H. & Miao, M. Simple Route to Metal cyclo-N_5^-

       Salt: High-Pressure Synthesis of CuN_5. *J Phys Chem C* **122**, 22339-22344

       (2018).

15   Steele, B. A. *et al.* High-pressure synthesis of a pentazolate salt. *Chem Mater*

       29, 735-741 (2016).

16   Laniel, D., Weck, G., Gaiffe, G., Garbarino, G. & Loubeyre, P. High-pressure

       synthesized lithium pentazolate compound metastable under ambient

       conditions. *J Phys Chem Lett* **9**, 1600-1604 (2018).

17   Xia, K. *et al.* Pressure-Stabilized High-Energy-Density Alkaline-Earth-Metal

Pentazolate Salts. *J Phys Chem C* 123, 10205-10211 (2019).

18   C. Yang, C. Zhang, Z. Zheng, C. Jiang, J. Luo, Y. Du, B. Hu, C. Sun and K. O.

Christe, *J. Am. Chem. Soc.* 140, 16488-16494 (2018).

19   Pickard, C. J. & Needs, R. High-pressure phases of nitrogen. *Phys. Rev. Lett.*

102, 125702 (2009).

20   Goncharov, A. F., Gregoryanz, E., Mao, H.-k., Liu, Z. & Hemley, R. J. Optical

evidence for a nonmolecular phase of nitrogen above 150 GPa. *Phys. Rev. Lett.*

85, 1262 (2000).

21   Eremets, M. *et al.* Structural transformation of molecular nitrogen to a single-

bonded atomic state at high pressures. *J Chem Phys* 121, 11296-11300 (2004).

22   Caracas, R. & Hemley, R. J. New structures of dense nitrogen: Pathways to the

polymeric phase. *Chem Phys Lett* 442, 65-70 (2007).

23   McMahan, A. & LeSar, R. Pressure dissociation of solid nitrogen under 1 Mbar.

Phys. Rev. Lett. 54, 1929 (1985).

24   Zahariev, F., Hu, A., Hooper, J., Zhang, F. & Woo, T. Layered single-bonded

nonmolecular phase of nitrogen from first-principles simulation. *Phys Rev B*

72, 214108 (2005).

25   Jordan, T. H., Smith, H. W., Streib, W. E. & Lipscomb, W. N. Single-Crystal

X-Ray Diffraction Studies of α-N_2 and β-N_2. *J Chem Phys* 41, 756-759 (1964).

26   Zunger, A. & Huler, E. Calculation of structural properties and vibrational

frequencies of α-and γ-N_2 crystals. *J Chem Phys* 62, 3010-3023 (1975).

27   Eremets, M., Gavriliuk, A. & Trojan, I. Single-crystalline polymeric nitrogen. *Appl Phys Lett* **90**, 171904 (2007).

28   Mailhiot, C., Yang, L. & McMahan, A. Polymeric nitrogen. *Phys Rev B* **46**, 14419 (1992).

29   Eremets, M. I., Gavriliuk, A. G., Trojan, I. A., Dzivenko, D. A. & Boehler, R. Single-bonded cubic form of nitrogen. *Nat. Mater.* **3**, 558-563 (2004).

30   Wang, X. *et al.* Cagelike diamondoid nitrogen at high pressures. *Phys. Rev. Lett.* **109**, 175502 (2012).

31   Laniel, D., Geneste, G., Weck, G., Mezouar, M. & Loubeyre, P. Hexagonal layered polymeric nitrogen phase synthesized near 250 GPa. *Phys. Rev. Lett.* **122**, 066001 (2019).

32   Ma, Y., Oganov, A. R., Li, Z., Xie, Y. & Kotakoski, J. Novel high pressure structures of polymeric nitrogen. *Phys. Rev. Lett.* **102**, 065501 (2009).

33   Li, Y. *et al.* Route to high-energy density polymeric nitrogen t-N via He-N compounds. *Nat. Commun.* **9**, 1-7 (2018).

34   Korkin, A. A., Balkova, A., Bartlett, R. J., Boyd, R. J. & Schleyer, P. v. R. The 28-electron tetraatomic molecules: N_4, CN_2O, BFN_2, C_2O_2, B_2F_2, CBFO, C_2FN, and BNO_2. Challenges for computational and experimental chemistry. *J Phys Chem* **100**, 5702-5714 (1996).

35   Li, Q. S. & Liu, Y. D. Theoretical studies of the N_6 potential energy surface. *J Phys Chem A* **106**, 9538-9542 (2002).

36 Trinquier, G., Malrieu, J.-P. & Daudey, J.-P. AB initio study of the regular polyhedral molecules N_4, P_4, As_4, N_8, P_8 and As_8. *Chem Phys Lett* **80**, 552-557 (1981).

37 Ren, Y. *et al.* Theoretical study of the N_{10} clusters without double bonds. *Int J Quantum Chem* **82**, 34-43 (2001).

38 Li, Q. S. & Zhao, J. F. Theoretical study of potential energy surfaces for N_{12} clusters. *J Phys Chem A* **106**, 5367-5372 (2002).

39 Guan, J., Zhang, S., Xu, W. & Li, Q. A Quantum Chemical Study of N_{14} Cluster. *Struct Chem* **15**, 121-132 (2004).

40 Strout, D. L. Cage isomers of N_{14} and N_{16}: nitrogen molecules that are not a multiple of six. *J Phys Chem A* **108**, 10911-10916 (2004).

41 Ha, T.-K., Suleimenov, O. & Nguyen, M. T. A quantum chemical study of three isomers of N_{20}. *Chem Phys Lett* **315**, 327-334 (1999).

42 Greschner, M. J. *et al.* A new allotrope of nitrogen as high-energy density material. *J Phys Chem A* **120**, 2920-2925 (2016).

43 Hirshberg, B., Gerber, R. B. & Krylov, A. I. Calculations predict a stable molecular crystal of N_8. *Nat Chem* **6**, 52 (2014).

44 Liu, S., Zhao, L., Yao, M., Miao, M. and Liu, B. Novel All-Nitrogen Molecular Crystals of Aromatic N_{10}. *Adv. Sci.* **7**, 1902320.

45 Wang, Y., Lv, J., Zhu, L. & Ma, Y. Crystal structure prediction via particle-swarm optimization. *Phys Rev B* **82**, 094116 (2010).

46   Wang, Y., Lv, J., Zhu, L. & Ma, Y. CALYPSO: A method for crystal structure

prediction. *Comput. Phys. Commun.* **183**, 2063-2070 (2012).

47   Kresse, G. & Hafner, J. Ab initio molecular-dynamics simulation of the liquid-

metal-amorphous-semiconductor transition in germanium. *Phys Rev B* **49**,

14251 (1994).

48   Kresse, G. & Furthmüller, J. Efficiency of ab-initio total energy calculations for

metals and semiconductors using a plane-wave basis set. *Comput Mater Sci* **6**,

15-50 (1996).

49   Perdew, J. P., Burke, K. & Ernzerhof, M. Generalized gradient approximation

made simple. *Phys. Rev. Lett.* **77**, 3865 (1996).

50   Kresse, G. & Joubert, D. From ultrasoft pseudopotentials to the projector

augmented-wave method. *Phys Rev B* **59**, 1758 (1999).

51   Blöchl, P. E. Projector augmented-wave method. *Phys Rev B* **50**, 17953 (1994).

52   Klimeš, J., Bowler, D. R. & Michaelides, A. Chemical accuracy for the van der

Waals density functional. *Journal of Physics: Condensed Matter* **22**, 022201

(2009).

53   Klimeš, J., Bowler, D. R. & Michaelides, A. Van der Waals density functionals

applied to solids. *Phys Rev B* **83**, 195131 (2011).

54   Togo, A., Oba, F. & Tanaka, I. First-principles calculations of the ferroelastic

transition between rutile-type and $CaCl_2$-type SiO_2 at high pressures. *Phys Rev

B* **78**, 134106 (2008).

55   M. J. Frisch, G. W. T., H. B. Schlegel, G. E. Scuseria,   *et al.* Gaussian 16

       Revision B.01. 2016; Gaussian Inc. *Wallingford CT* (2016).

56   Becke, A. D. Density-functional thermochemistry. III. The role of exact

       exchange. *J Chem Phys* **98**, 5648-5652 (1993).

57   A., P. G. *et al.* A complete basis set model chemistry. I. The total energies of

       closed-shell atoms and hydrides of the first-row elements. *J Chem Phys* **89**,

       2193-2218 (1988).

58   Petersson, G. & Al-Laham, M. A. A complete basis set model chemistry. II.

       Open-shell systems and the total energies of the first-row atoms. *J Chem Phys*

       94, 6081-6090 (1991).

59   Glukhovtsev, M. N., Jiao, H. & Schleyer, P. v. R. Besides N_2, what is the most

       stable molecule composed only of nitrogen atoms? *Inorg Chem* **35**, 7124-7133

       (1996).

60   Chen, C. & Sun, K. C. Comparisons of the theoretical calculation of nitrogen

       clusters by semiempirical MO method. *Int J Quantum Chem* **60**, 1709-1718

       (1996).

61   Mull, H. F., Turney, J. M., Douberly, G. E. and Schaefer III, H. F. Kinetic

       Stability of Pentazole. *J. Phys. Chem. A* **125**, 9092-9098(2021).